How stress can reduce dissipation in glasses

Jiansheng Wu and Clare C. Yu

Department of Physics and Astronomy, University of California, Irvine, California 92697, USA
(Received 4 October 2011; published 21 November 2011)

We propose that stress can decrease the internal friction of amorphous solids, either by increasing the potential barriers of defects, thus reducing their tunneling and thermal activation that produce loss, or by decreasing the coupling between defects and phonons. This stress can be from impurities, atomic bonding constraints, or externally applied stress. Externally applied stress also reduces mechanical loss through dissipation dilution. Our results are consistent with the experiments, and predict that stress could substantially reduce dielectric loss and increase the thermal conductivity.

I. INTRODUCTION

At low temperatures between 0.1 and 10 K, a wide variety of amorphous solids exhibit a universal plateau in their mechanical dissipation $Q^{-1} \sim 10^{-4}$–10^{-3}.[1,2] However, there are exceptions such as in amorphous silicon where doping with 1 at. % of hydrogen reduces the low-temperature internal friction plateau by about a factor of 200.[3] In addition, the dissipation in high-stress silicon nitride (Si_3N_4) thin films, which show no long-range order in x-ray diffraction and TEM images, is two to three orders of magnitude lower than in amorphous SiO_2 from 4 K up to room temperature.[4] Such a large effect is surprising since the stress of 1.2 GPa corresponds to only about 70 K/atom. Even the dissipation of stress-relieved Si_3N_4 has a Q^{-1} that is about an order of magnitude lower than typical amorphous solids.[4]

So far no theoretical explanation for these results has been presented. In this paper we propose that all these reductions in dissipation are due to stress but cannot be explained by one physical effect. Impurities, dopants, and internal bond constraints can produce internal stress. Externally applied stress can reduce dissipation through dissipation dilution[5] as Saulson has pointed out.[6] In addition we propose that stress, whether internal or external, can reduce the dissipation produced by microscopic defects known as two-level systems (TLS), either by increasing TLS barrier heights or by decreasing the coupling between phonons and TLS. Our goal is to urge experimentalists to make further measurements to quantify the role of dissipation dilution as well as to differentiate between these two possible effects of stress on TLS.

In dissipation dilution[7] externally applied stress increases the stiffness of materials without increasing their loss, resulting in a higher Q. A simple example of dissipation dilution would be the increase in Q of a mass suspended from a lossy spring when a stiffer lossless spring is added in parallel to the original spring. Since $Q = f_0/(\Delta f)$ where f_0 is the resonant frequency and Δf is the linewidth (full width at half maximum), f_0, and hence Q, increase without increasing the damping. In the Appendix we estimate that a thin-film square resonator of high-stress silicon nitride could have a Q up to 40 000 times higher than a hypothetical stress-relieved silicon nitride resonator due to dissipation dilution. This far exceeds the experimental factor of order 150 by which external stress increases Q in high-stress silicon nitride.[4] The full enhancement of 40 000 is not realized,

probably due to external sources of dissipation, e.g., clamping losses.

Dissipation dilution only plays a role when there is externally applied stress. So even though dissipation dilution can have a dramatic effect, it cannot explain why dissipation is lowered by an order of magnitude or more in materials which have no externally applied stress, e.g., in silicon doped with 1 at. % hydrogen[3] or in stress-relieved Si_3N_4.[4] Also, in addition to dissipation dilution, external stress may reduce the internal friction arising from microscopic defects. To understand this, we note that $Q^{-1} = A\phi$ where ϕ is internal friction, and A is due to dissipation dilution and is a function of macroscopic parameters, e.g., elastic moduli.[7] (For the rest of the paper, except where noted otherwise, we will focus on the internal friction and set $A = 1$ so that we can use Q^{-1} in place of ϕ in order to be consistent with the accepted notation in the field of glasses at low temperatures.) We propose two possible ways in which stress could reduce internal friction: either by increasing the barrier heights of microscopic fluctuating defects or by decreasing the coupling (deformation potential γ) between phonons and TLS. We fit existing, but incomplete, experimental data on dissipation, specific heat, and thermal conductivity for silicon nitride and SiO_2, finding somewhat better fits to the Q^{-1} data of Si_3N_4 at high temperatures with the barrier height model. Further measurements could distinguish between these two models.

In glasses at low temperatures, acoustic loss at low frequencies is attributed to TLS.[2,8–12] While the microscopic nature of TLS is a mystery, one can think of a TLS as an atom or group of atoms in a double-well potential that can sit in either well. At low temperatures, the lowest two energy levels dominate. The TLS density of states is assumed to be uniform at energies below a few Kelvin, so if stress merely shifts the density of states, there should be no effect. At low frequencies and temperatures, the primary mode of attenuation is relaxation in which the phonon at the measurement frequency modulates the TLS energy-level spacing.[13] The measurement frequency is not related to the TLS energy because the incident phonon can modulate TLS with any energy splitting. Attenuation occurs when the TLS population readjusts to the equilibrium Boltzmann distribution with the aid of the entire thermal distribution of phonons.

Low acoustic loss could have important implications for dielectric loss since the two are completely analogous within

the TLS model.[14] TLS with electric dipole moments can produce dielectric loss by attenuating photons. So we would expect stressed dielectrics to also have low dielectric loss that could make them useful substrates to reduce loss and noise in superconducting qubit circuits.[15] For example, hydrogenating amorphous silicon nitride decreases its dielectric loss tangent by approximately a factor of 50.[16]

At low temperatures tunneling dominates, but at higher temperatures thermal activation over energy barriers becomes important. One possibility is that stress increases the potential energy barriers V, which reduces tunneling and thermal activation, thus effectively reducing the number of defects and the internal friction. We will show that this approach is quantitatively consistent with measurements of Q^{-1} in stress-relieved Si_3N_4, and, even if we ignore dissipation dilution and demand that the entire reduction be due to a reduction in internal friction, with measurements of Q^{-1} in high-stress Si_3N_4. We use a single set of parameters to calculate Q^{-1}, the specific heat $C(T)$, and the thermal conductivity $\kappa(T)$ in SiO_2 and silicon nitride. Since low dissipation implies a long phonon mean-free path and a high thermal conductivity, we predict that the thermal conductivity of stress-relieved Si_3N_4 is an order of magnitude higher than amorphous SiO_2 from 4 K up to room temperature, and, if there is no dissipation dilution, the thermal conductivity of high-stress Si_3N_4 could be even higher, potentially making silicon nitride a useful substrate for integrated circuits where cooling is important.

The paper is organized as follows. We describe our calculations of the dissipation, thermal conductivity, specific heat, and dielectric loss in Sec. II. In Sec. III, we explain our procedure for determining the parameters for fitting the experimental data. The results of those fits to the specific heat, thermal conductivity, and dissipation are presented in Sec. IV. We discuss why the dissipation of stress-relieved Si_3N_4 is lower than ordinary materials in Sec. V. We discuss the possibility that stress could reduce dielectric loss in Sec. VI. In Sec. VII we present an alternative model for how stress could lower the dissipation, namely, by reducing the coupling between TLS and phonons. We summarize our work in Sec. VIII.

II. CALCULATIONS OF DISSIPATION, THERMAL CONDUCTIVITY, SPECIFIC HEAT, AND DIELECTRIC LOSS

Let us briefly review the TLS model.[8,9] The TLS Hamiltonian is $H = H_0 + H_e$, where $H_0 = (1/2)[\Delta\sigma_z - \Delta_0\sigma_x]$ and $H_e = \gamma e\sigma_z$, where Δ is the energy asymmetry between the potential energy wells, Δ_0 is the tunneling matrix element, γ is the deformation potential, e is the strain field, and σ_x and σ_z are Pauli matrices. The energy eigenvalues of H_0 are $E = \pm\sqrt{\Delta_0^2 + \Delta^2}$. We follow Tielburger *et al.*[17] and approximate the double well by two overlapping harmonic oscillator wells, each with energy-level spacing $\hbar\Omega_0$. The tunneling matrix element Δ_0 is given by the WKB approximation:[17]

$$\Delta_0 = \frac{\hbar\Omega_0}{\pi}(\sqrt{\Lambda+1} + \sqrt{\Lambda})\exp(-\sqrt{\Lambda^2 + \Lambda}), \quad (1)$$

where $\Lambda = 2V/(\hbar\Omega_0)$ and V is the height of the energy barrier. Fits to the low-temperature thermal conductivity find the TLS

density of states $\bar{P}$ that couples to phonons to be approximately constant. However, an excess of local vibrational states, referred to as the boson peak, is evident at higher temperatures and energies.[1,18] We model these modes by Einstein oscillators with a step function in the density of states that starts at an energy E_0 typically between 10 and 40 K.[19]

According to the TLS model, at low frequencies ($\nu < 1$ THz) and low temperatures (0.1 K $< T <$ 10 K), Q^{-1} is a temperature-independent constant given by[10]

$$Q_0^{-1} = \frac{\pi\bar{P}\gamma^2}{2\rho v^2}, \quad (2)$$

where ρ is the mass density, and v is the sound velocity. The sources of attenuation are TLS relaxation processes ($Q_{rel,TLS}^{-1}$), resonant scattering of phonons from TLS ($Q_{res,TLS}^{-1}$) and Einstein oscillators (Q_{EO}^{-1}) in which the phonon energy matches the energy-level spacing, and Rayleigh scattering (Q_{Ray}^{-1}) from small scatterers of size a such that $ka \stackrel{<}{\sim} 1$, where k is the phonon wave vector.[19] Yu and Freeman[19] found that $a = k^{-1} = \hbar v/E_0$ is consistently $\sim$25% larger than the size[20] of a molecular unit for SiO_2, GeO_2, polystyrene, and PMMA (polymethylmethacrylate). Just as in their work, we cut off Rayleigh scattering at E_0. We include thermal activation as well as direct phonon relaxation in the TLS relaxation processes,[17] and assume that the relaxation attenuation from Einstein oscillators is negligible.[19] Thus we can write[17,19]

$$Q^{-1} = \begin{cases} Q_{res,TLS}^{-1} + Q_{rel,TLS}^{-1} + Q_{Ray}^{-1}, & E < E_0 \\ Q_{res,TLS}^{-1} + Q_{rel,TLS}^{-1} + Q_{EO}^{-1}, & E > E_0. \end{cases} \quad (3)$$

The attenuation due to TLS relaxation is given by

$$Q_{rel,TLS}^{-1} = \frac{2Q_0^{-1}}{\pi k_B T}\int_{V,\Delta}\left(\frac{\Delta}{E}\right)^2 \text{sech}^2\frac{E}{2k_B T}\frac{\omega\tau}{1+(\omega\tau)^2}, \quad (4)$$

where $\int_{V,\Delta} \equiv \int_0^{V_{max}} dV \int_0^{2V} d\Delta\, P(\Delta,V)/\bar{P}$ with $V_{max} = V_0 + 6\sigma_0$. $P(\Delta,V)$ is the TLS distribution of Δ and V. We assume that Δ has a uniform distribution and V has a Gaussian distribution with an average V_0 and a variance σ_0^2:[17]

$$P(\Delta,V) = \frac{2\bar{P}}{\hbar\Omega_0}\exp\left[-\frac{(V-V_0)^2}{2\sigma_0^2}\right]. \quad (5)$$

The TLS relaxation rate τ^{-1} is the sum of the direct phonon relaxation rate τ_d^{-1}, in which the excited TLS decays to the ground state by emitting a phonon, and the rate τ_{Arr}^{-1} of Arrhenius activation over the barrier:

$$\tau^{-1} = \tau_d^{-1} + \tau_{Arr}^{-1}, \quad (6)$$

$$\tau_d^{-1} = \sum_{a=\ell,t}\left(\frac{\gamma_a^2}{v_a^5}\right)\frac{E\Delta_0^2}{2\pi\rho\hbar^4}\coth\left(\frac{E}{2k_B T}\right), \quad (7)$$

$$\tau_{Arr}^{-1} = \tau_0^{-1}\cosh\left(\frac{\Delta}{2k_B T}\right)e^{-V/k_B T}, \quad (8)$$

where the sum is over the longitudinal and transverse phonon modes and $\tau_0 = 2/\Omega_0$. For SiO_2, $\tau_0 = 4\times 10^{-12}$ s. For $\omega\tau_m \ll 1$, $Q_{rel,TLS}^{-1} \approx Q_0^{-1}$, where τ_m is the minimum relaxation time for a TLS with energy E at temperature T.[19]

The Rayleigh and resonant phonon scattering terms are given by

$$Q_{\text{Ray}}^{-1} = Bv\omega^3, \qquad (9)$$

$$Q_{\text{EO}}^{-1} = Q_0^{-1}\frac{2S_\kappa}{\pi}, \qquad (10)$$

$$Q_{\text{res,TLS}}^{-1} = 2Q_0^{-1}\int_{V,\Delta}\tanh\frac{\hbar\omega}{k_B T}\left(\frac{\Delta_0}{E}\right)^2\delta(E-\hbar\omega), \qquad (11)$$

where S_κ is the step height in the density of states of the Einstein oscillators that is used to fit the thermal conductivity κ, and B is a constant.

Q^{-1} is measured at low frequencies of order 1 MHz. Estimating the order of magnitude of the various contributions at 1 MHz and 1 K using the values of the parameters in Table I for SiO$_2$ (transverse phonon modes), we find $Q_{\text{rel,TLS}}^{-1} \sim Q_0^{-1} \sim 6\times10^{-4}$, $Q_{\text{res,TLS}}^{-1} \sim Q_0^{-1}\tanh(\hbar\omega/2k_B T)\sim 1\times10^{-8}$, and $Q_{\text{Ray}}^{-1}\sim 2\times10^{-15}$. Thus TLS relaxation dominates Q^{-1} at low temperatures and low frequencies where the plateau in Q^{-1} is given by

$$Q_{\text{plat}}^{-1} = Q_0^{-1}\exp\left[-\frac{V_0^2}{2\sigma_0^2}\right]. \qquad (12)$$

This replaces Eq. (2), and is obtained by plugging Eq. (4) into Eq. (3) and noting that the dominant contribution to the integral in Eq. (3) is for $V \ll V_0$ due to the exponential dependence of τ_{Arr}^{-1} and τ_d^{-1} on V. The factor of $\exp[-(V_0/\sigma_0)^2]$ in $P(\Delta,V)$ effectively reduces the number of active TLS.

The relaxation time τ in Eq. (4) for $Q_{\text{rel,TLS}}^{-1}$ is exponentially sensitive to the barrier height V because both the tunneling matrix element Δ_0 in τ_d [see Eqs. (1) and (7)] and the thermal activation time τ_{Arr} given by Eq. (8) depend exponentially on V. We assume that stress increases the barrier heights V, thus increasing the relaxation times τ_d and τ_{Arr}, and reducing the dissipation $Q^{-1}\approx Q_{\text{rel,TLS}}^{-1}$. In our model stress increases the average barrier height V_0 and decreases the variance σ_0^2 in $P(\Delta,V)$.

In order to determine the values of the parameters required to fit Q^{-1}, we need to fit the thermal conductivity $\kappa(T)$ and the specific heat $C(T)$. The equations for $C(T)$ and $\kappa(T)$ are as follows. In glasses heat is carried by phonons.[21] $\kappa(T)$ is given by

$$\kappa(T) = \frac{1}{3}\int_0^{\omega_D} C_D(T,\omega)v\ell(T,\omega)d\omega, \qquad (13)$$

where ω_D is the Debye frequency, and we approximate the phonon specific heat by the Debye specific heat $C_D(T,\omega)$. The phonon mean-free path ℓ is related to Q by

$$\ell(T,\omega) = Q(T,\omega)v/\omega = Q(T,\omega)\lambda/(2\pi), \qquad (14)$$

where λ is the phonon wavelength.

The specific heat $C(T)$ has contributions from the phonons which we approximate with the Debye specific heat C_D, from TLS C_{TLS}, and from local modes which we model with Einstein oscillators C_{EO}:[19]

$$C(T) = C_D(T) + C_{\text{TLS}}(T) + C_{\text{EO}}(T), \qquad (15)$$

where

$$C_D = 9\frac{N}{V}k_B\left(\frac{T}{\Theta_D}\right)^3\int_0^{x_D}dx\,4x^4\frac{e^x}{(e^x-1)^2}, \qquad (16)$$

$$C_{\text{TLS}} = k_B\bar{P}\int_{V,\Delta}x^2\frac{e^x}{(e^x+1)^2} = \frac{\pi^2}{6}n_0k_B^2T, \qquad (17)$$

$$C_{\text{EO}} = n_0 S_c k_B^2 T\int_{x_0}^{x_D}dx\frac{x^2e^x}{(e^x-1)^2}, \qquad (18)$$

where $x = E/k_B T$, $x_0 = \hbar\Omega_0/k_B T$, $x_D = \Theta_D/T$, N/V is the number density of formula units, and $\theta(E)$ is a step function. Θ_D is the Debye temperature. n_0 is the TLS density of states

TABLE I. Parameters for SiO$_2$, A (200-nm-thick SiN$_{1.15}$), B (50-nm-thick SiN$_{1.15}$), and Si$_3$N$_4$.

Quantities[a]	SiO$_2$	A	B	Si$_3$N$_4$[b]
ρ (10^3 kg/m^3)	2.2	2.68	2.68	3.18
v_L (10^3 m/s)[c]	5.8(L) 3.75(T)	11.0	11.7	11.17
Θ_D (K)	342	610	649	446
E_0 (K)	43	76	81	56
$\bar{P}$ (10^{45}/J m^3)	0.16	3	10	$\sim$0.39
S_c	1300	7.0	2.0	7.0*
S_κ	250	2.5	1.5	2.5*
B (10^{-43} s^4/m)	1.7×10^4	8	6	8*
γ (eV)	2.24(L) 1.73(T)	5.6	5.6	5.6*
$\hbar\Omega_0$ (K)	12	150	150	150/130
$2Q_0^{-1}/\pi$ (10^{-3}) (L)	0.28	68	114	2.13
n_0 (10^{45}/J m^3)	2.1	448	1490	58.3/56.4
$n_0\times 10$ K/(N/V) (10^{-3})	1.31×10^{-2}	1.7	5.6	0.59/0.57
V_0 ($\times10^4$ K)	0	2.3	2.3	2.3/3.05
σ_0 ($\times10^3$ K)	0.445	9	9	9/7.5

[a]Density ρ and sound velocity v are from Refs. 4 and 25. Θ_D is calculated from ρ and v.

[b]Parameters marked with * for Si$_3$N$_4$ are estimated from SiN$_{1.15}$ and SiO$_2$, while those marked with $\sim$ are estimated from other materials. Stress-relieved and high-stress values for Si$_3$N$_4$ are separated by / with stress-relieved values given first.

[c]L (T) stands for longitudinal (transverse) components. If no data is available, we use $v_T \approx v_L/2$.

that contributes to the specific heat, and S_C is the size of the step in the density of states due to the Einstein oscillators that contribute to $C(T)$.

The dielectric loss tangent $\tan \delta$ is analogous to the acoustic dissipation Q^{-1}. At high frequencies and low temperatures ($\lesssim 1$ K), the dominant scattering is resonant scattering of photons by TLS in which the photon energy matches the TLS energy splitting. If the electromagnetic intensity J is much less than the critical intensity J_c, we are below saturation and can use Eq. (11) with $\tan \delta$ replacing $Q_{\rm res,TLS}^{-1}$, and Q_0^{-1} replaced by[22]

$$Q_{0,\rm dielectric}^{-1} = \frac{4\pi^2 n_e p^2}{3\varepsilon_0 \varepsilon_r}, \tag{19}$$

where n_e is the density of TLS with electric dipole moments, p is the electric dipole moment, ω is the angular frequency of the incident photons, ε_0 is the permittivity of the vacuum, and ε_r is the dielectric constant. Since the integral in Eq. (11) is dominated by $V \ll V_0$, we can make the approximation

$$\tan \delta = Q_{0,\rm dielectric}^{-1} \exp\left[-\frac{V_0^2}{2\sigma_0^2}\right] \tanh\left(\frac{\hbar\omega}{2k_B T}\right) \tag{20}$$

for the barrier height model. For the model, described in Sec. VII, where the stress modifies the deformation potential γ, $V_0 = 0$, and

$$\tan \delta = Q_{0,\rm dielectric}^{-1} \tanh\left(\frac{\hbar\omega}{2k_B T}\right). \tag{21}$$

III. PROCEDURE FOR FITTING THE EXPERIMENTAL DATA

A. SiO₂

To fit the data for SiO_2 we follow Tielburger *et al.*[17] and set $V_0 = 0$. Then by fitting the low-temperature plateau of Q^{-1} using Eqs. (2) and (12), we obtain $\bar{P}\gamma^2$. Fitting Q^{-1} over the whole range of temperature yields σ_0. The temperature of the rise in Q^{-1} determines $\hbar\Omega_0/2$. Since V_0 and σ_0 are known, we can determine n_0 by fitting the specific heat $C(T)$ which then gives the value of $\bar{P}$. $\bar{P}$, γ, V_0, and σ_0 determine the low-temperature thermal conductivity $\kappa(T)$ without any adjustable parameters. We set the energy E_o of the onset of the step in the density of states by $E_0 = \Theta_D/(2\pi \times 1.27)$,[19] where Θ_D is the Debye temperature. Fitting $C(T)$ at higher temperatures determines the step S_C in the density of states due to local modes (Einstein oscillators). The fit to $\kappa(T)$ at high temperatures gives the step in the density of states S_κ and the Rayleigh scattering parameter B. Note that $\bar{P} < n_0$ and $S_\kappa < S_C$ because not all of the degrees of freedom that contribute to the specific heat scatter the phonons that are responsible for the thermal conductivity. No one has tried before to see if one set of parameters can be used to fit the data for all these quantities.

B. Si₃N₄

Fitting the data for Si_3N_4 is complicated by the fact that measurements of $Q^{-1}(T)$, $\kappa(T)$, and $C(T)$ have not been made for the same stoichiometry of silicon nitride. We assume a $\bar{P}\gamma^2$ value (such that $Q_0^{-1} \approx 10^{-4}$–10^{-3}) for Si_3N_4 and use Eq. (12) to fit the $Q^{-1}(T)$ data for low-stress Si_3N_4 (Ref. 4) to obtain V_0

and σ_0. Assuming $SiN_{1.15}$ has the same values of V_0 and σ_0 as low-stress Si_3N_4, we can obtain n_0 and $\bar{P}$ by fitting the $C(T)$ data of $SiN_{1.15}$. By fitting the $\kappa(T)$ data of $SiN_{1.15}$, we obtain $\bar{P}\gamma^2$, and thus γ. Assuming Si_3N_4 has the same γ as $SiN_{1.15}$, we obtain $\bar{P}$ for Si_3N_4. If this value is reasonable compared to the γ values for $SiN_{1.15}$ and a-SiO_2, we stop. Otherwise, we choose another $\bar{P}\gamma^2$ and repeat the above procedure until we obtain a reasonable value of $\bar{P}$. We then follow the procedure given in the previous paragraph to fit $C(T)$ and $\kappa(T)$ for $SiN_{1.15}$ at higher temperatures to obtain the values of B, S_κ, and S_C.

IV. RESULTS: FITS TO EXPERIMENTAL DATA

A. SiO₂

Our fits to the data for $\kappa(T)$, $C(T)$, and Q^{-1} for SiO_2 and silicon nitride are shown in Figs. 1, 2, and 3 with the parameters given in Table I. No one has tried before to see if one set of parameters can be used to fit the data for all these quantities. The fits to the SiO_2 data show that this can be done.

Fefferman *et al.*[23] have reported that around 10 mK, the acoustic dissipation of SiO_2 is linear in temperature. This linear temperature dependence is attributed to interactions between TLS.[23] In Fig. 4 we show our fits to the data from Ref. 23. To obtain these fits we followed Fefferman *et al.*[23] and added a linear term $\tau_{\rm int} = bT(\Delta_0/E)^2$,[24] where b is a constant to the expression for the relaxation rates in Eq. (6). b is a constant.

B. Si₃N₄

Fitting the data for Si_3N_4 is complicated by the fact that measurements of $Q^{-1}(T)$, $\kappa(T)$, and $C(T)$ have not been made
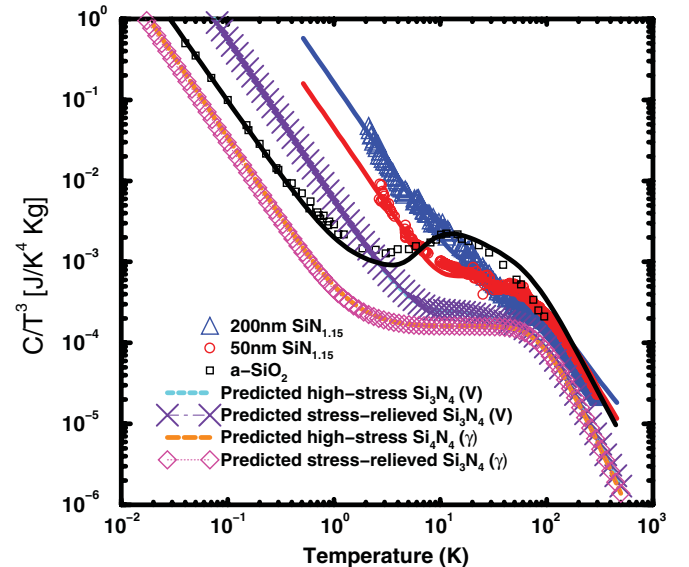

FIG. 1. (Color online) $C(T)/T^3$ vs T for amorphous SiO_2 and silicon nitride. Experimental data points are shown for 50- and 200-nm-thick $SiN_{1.15}$ (Ref. 25) and SiO_2. The SiO_2 $C(T)$ data are from Refs. 1 and 26. The solid lines through the points are theoretical fits. Our predictions where stress affects V or γ are indicated in the legend by (V) and (γ), respectively. $C(T)/T^3$ curves for high-stress and stress-relieved Si_3N_4 lie on top of each other for the barrier height model and similarly for the γ model.
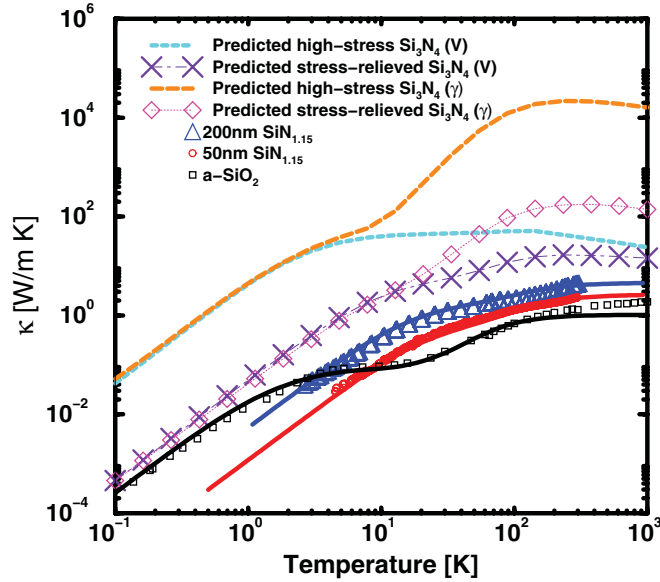
FIG. 2. (Color online) $\kappa(T)$ vs T for amorphous SiO_2 and silicon nitride. Experimental data points are shown for 50- and 200-nm-thick $SiN_{1.15}$ (Ref. 25) and SiO_2. The SiO_2 $\kappa(T)$ data are from Refs. 27 and 28. The solid lines through the points are theoretical fits. Our predictions where stress affects V or γ are indicated in the legend by (V) and (γ), respectively. At low temperatures $\kappa(T)$ for high-stress Si_3N_4 is the same for the V and γ models and similarly for stress-relieved Si_3N_4.

for the same stoichiometry of silicon nitride. Assuming that $Q^{-1} = \phi$, i.e., with no dissipation dilution, our predictions for $C(T)$ and $\kappa(T)$ for high-stress and stress-relieved Si_3N_4 are shown in Figs. 1 and 2. Around 3 K, $\kappa(T)$ for stress-relieved Si_3N_4 is about an order of magnitude higher than for SiO_2, and
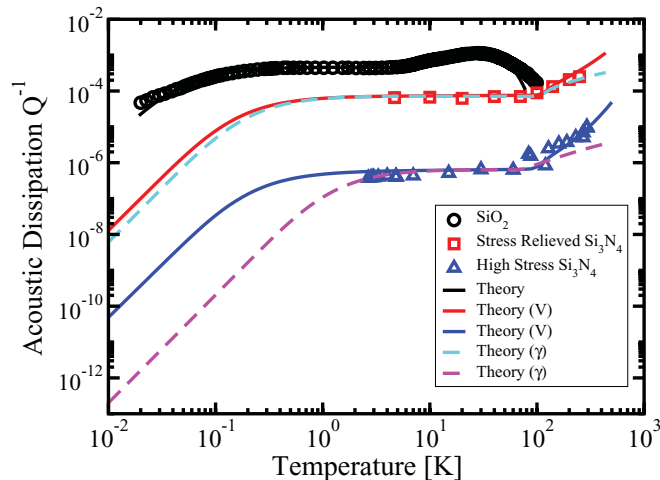

FIG. 3. (Color online) Dissipation Q^{-1} vs T for stress-relieved Si_3N_4 measured at 3.5387 MHz (open squares) (Ref. 4), high-stress Si_3N_4 measured at 1.526 445 MHz (open triangles) (Ref. 4), and amorphous SiO_2 (open circles) measured at 11.4 kHz (Ref. 17). Solid lines are theoretical fits using the model where stress reduces barrier height. Dashed lines are our theoretical predictions associated with reducing γ. Dissipation dilution factor $A = 1$ in the theoretical curves.
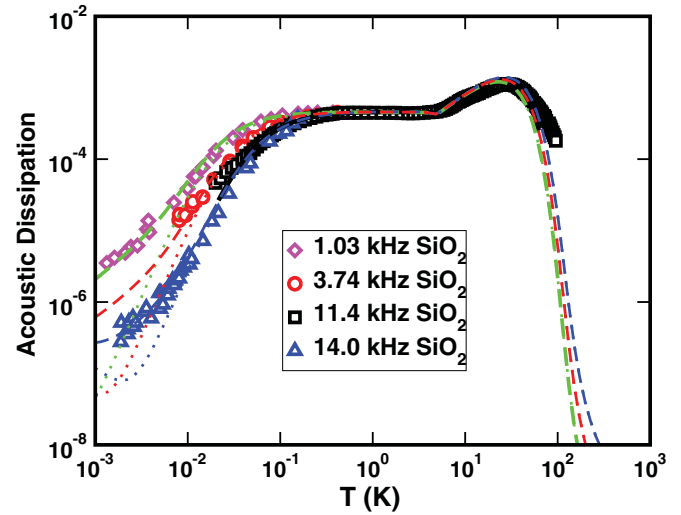

FIG. 4. (Color online) Acoustic dissipation Q^{-1} vs temperature for SiO_2 at various frequencies. The data for SiO_2 at 11.4 kHz is from Ref. 17, while the rest of the SiO_2 data is from Ref. 23. The fits to the SiO_2 data with the linear term bT are given by dashed lines, while the fits without the linear term added are shown as dotted lines.

high-stress Si_3N_4 could be even higher, which is consistent with low dissipation and a long phonon mean-free path.

From Table I, we see that our fits to $C(T)$ for $SiN_{1.15\pm0.05}$ require surprisingly large values of n_0, the TLS density of states; $n_0 = 4.5 \times 10^{47}/J\,m^3$ for 200-nm-thick films and $n_0 = 1.5 \times 10^{48}/J\,m^3$ for 50-nm-thick films, which are two and three orders of magnitude larger than values for amorphous SiO_2, respectively. This accounts for the high specific heat below 5 K.

Our model fits the Q^{-1} data very well. At low temperatures ($T < 0.1$ K), $Q^{-1} \sim T^3$, and we predict that Q will increase by up to an order of magnitude from 400 to 100 mK in both stress-relieved and high-stress Si_3N_4. To obtain an upper bound for the change in barrier height due to stress, we ignore dissipation dilution. In this case from Table I we see that the mean barrier height for high-stress Si_3N_4 is $V_0 = 3.05 \times 10^4$ K ~ 2.6 eV, which is about 33% higher than $V_0 = 2.3 \times 10^4$ K ~ 2 eV for stress-relieved Si_3N_4. These values are comparable to the bond energies of Si_3N_4.[29] This increase in V_0 is consistent with our hypothesis that stress increases the barrier heights. To see that these numbers are reasonable, note that the difference ΔV_0 in mean barrier height V_0 due to stress is 7500 K. The applied stress is estimated to be about 70 K/atom. $n_0 \times 10$ K/(N/V) in Table I implies that 0.06% or 1 in 1700 atoms are fluctuating defects. If the stress is distributed nonuniformly so that each atom contributes, say, 6% of its stress to the defect, then 70 K/atom $\times$ 1700 atoms $\times$ 6% = 7100 K $\sim \Delta V_0$.

V. DISSIPATION OF STRESS-RELIEVED Si_3N_4

Why is Q^{-1} in stress-relieved Si_3N_4 an order of magnitude lower than SiO_2?

One might naively expect stiffer materials to have less dissipation by looking at Eq. (2) and noticing that stiffer materials will have a higher speed v of sound. This is certainly true if we compare Si_3N_4 and SiO_2. A measure of the stiffness

of a material is the Young's modulus E. Silicon nitride has $E = 300$ GPa and $v = 11.7$ km/s, while SiO_2 is less stiff and has $E = 66$ GPa and $v = 5.8$ km/s. (We use longitudinal speeds of sound.) However, $\bar{P}\gamma^2$ can vary from material to material and seems to be larger in stiffer materials. For example, PMMA is much softer than SiO_2 with a Young's modulus E between 1.8 and 3.1 GPa. $\bar{P}\gamma^2$ for PMMA is about an order of magnitude smaller than the value for SiO_2,[19] but the values of their low-temperature dissipation Q^{-1} are comparable. ($\bar{P}\gamma^2 \sim 0.16 \times 10^7$ J/m³ for PMMA, and 1.6×10^7 J/m³ for SiO_2.)

As another example, consider SiO_2 and GeO_2. GeO_2 is softer than SiO_2; the Young's modulus $E = 45$ GPa for GeO_2 and $E = 66$ GPa for SiO_2 but the two materials have very comparable values of the dissipation plateau at 1 K: $Q^{-1} \sim 4 \times 10^{-4}$ for GeO_2 and $Q^{-1} \sim 5 \times 10^{-4}$ for SiO_2.[2] $\bar{P}\gamma^2 = 1.6 \times 10^7$ J/m³ for SiO_2 is double that of GeO_2, which has $\bar{P}\gamma^2 = 0.86 \times 10^7$ J/m³,[19] while $\rho v^2 \sim 37 \times 10^6$ J/m³ for SiO_2, which is about 50% larger than $\rho v^2 \sim 24 \times 10^6$ J/m³ for GeO_2. In short, the only way to determine the correct value of $\bar{P}$ and γ is to measure thermal conductivity, specific heat, and dissipation for samples of silicon nitride with the same stoichiometry. Stiffness alone is not enough to determine the parameters entering into the expression for the dissipation, or to account for the reduction in dissipation of stress-relieved Si_3N_4.

So we are still left with the question of why the dissipation of Si_3N_4 is an order of magnitude less than SiO_2. The reason is that the atomic bonds are more constrained in Si_3N_4. The competition between degrees of freedom and bond constraints is the reason why some materials are good glass formers and others are not.[30] Each m-fold coordinated atom provides $m/2$ constraints from fixed bond lengths, and $(2m - 3)$ constraints from fixed bond angles.[30] Since Si_3N_4 has three- and fourfold coordinated atoms, there are $5\frac{4}{7}$ constraints per atom, which exceeds the three degrees of freedom per atom. This is more constrained than SiO_2, which has $3\frac{2}{3}$ constraints per atom. This increase in the number of constraints reduces the number of defects (TLS) and produces unrelieved stress that increases the average barrier height, thus decreasing $C(T)$ and Q^{-1}, as well as increasing $\kappa(T)$.

VI. DIELECTRIC LOSS

As we mentioned in the Introduction, the dielectric loss tangent $\tan\delta$ is analogous to the acoustic dissipation Q^{-1}. So if stress reduces Q^{-1}, it should also reduce $\tan\delta$. We can estimate the effect of stress on $\tan\delta$ using the expression in the Appendix. For SiO_2 with $n_e p^2 = 1.46 \times 10^{-4}$,[22] $V_0 = 0$, and $\varepsilon_r = 3.9$, $Q^{-1}_{0,\text{dielectric}} \exp[-V_0^2/(2\sigma_0^2)] = Q^{-1}_{0,\text{dielectric}} \sim 5 \times 10^{-4}$. For Si_3N_4 with $\varepsilon_r = 7$,[31] and assuming n_e is given by $\bar{P}$ in Table I, $p = 1$ D, and using the values for V_0 and σ_0 from Table I, $Q^{-1}_{0,\text{dielectric}} \sim 7 \times 10^{-5}$ and $Q^{-1}_{0,\text{dielectric}} \exp[-V_0^2/(2\sigma_0^2)] \sim 3 \times 10^{-6}$ for stress-relieved Si_3N_4 and 2×10^{-8} for high-stress Si_3N_4. Thus stress-relieved Si_3N_4 has the potential to lower the dielectric loss by two orders of magnitude, and high-stress Si_3N_4 could have dielectric loss that is up to four orders of magnitude lower than SiO_2.

VII. ALTERNATIVE MODEL: REDUCED COUPLING γ BETWEEN TLS AND PHONONS

Our proposal that stress reduces the internal friction by increasing barrier heights can be made quantitatively consistent with the data. However, there are other possible explanations. One is that stress decreases the TLS-phonon coupling γ, and does not change the barrier height distribution. Figs. 1, 2, and 3 show the results of this approach with $V_0 = 0$, $\sigma_0 = 9000$ K, $\bar{P} = 4.3 \times 10^{43}/\text{J m}^3$, and $\gamma = 0.37$ (3.96) eV for high-stress (stress-relieved) Si_3N_4. The rest of the parameters are given in Table I for Si_3N_4. The Q^{-1} fit to stress-relieved Si_3N_4 is reasonably good, but poor for high-stress Si_3N_4 at high temperatures, indicating that this model does not work as well as our hypothesis that stress increases barrier heights if dissipation dilution plays no role. However, it is possible that some other set of values for the parameters could improve the fit to the dissipation of high-stress Si_3N_4. The predicted $C(T)$ and $\kappa(T)$ resulting from decreasing γ is shown in Figs. 1 and 2 for both high-stress and stress-relieved Si_3N_4. Reducing γ produces a thermal conductivity that is about the same as that of the barrier height model up to about 4 K and then, at high temperatures, is greater than that of the barrier height model by an order of magnitude or more. The specific heat associated with reducing γ is about two orders of magnitude lower than that of the barrier height model at low temperatures. If stress reduces γ, the dielectric loss will be the same for high-stress and stress-relieved Si_3N_4 with $Q^{-1}_{0,\text{dielectric}} \sim 7 \times 10^{-5}$. The dielectric loss for SiO_2 will be the same as in the barrier height model.

The way to differentiate between these models and to determine the role of dissipation dilution is to measure $C(T)$, $\kappa(T)$, Q^{-1}, and $\tan\delta$ for high-stress and stress-relieved Si_3N_4, and determine consistent values of the parameters $\bar{P}$, γ, V_0, and σ_0. If dissipation dilution is the sole cause of the reduction of dissipation by externally applied stress in high-stress Si_3N_4, the thermal conductivity, specific heat, and dielectric loss of high-stress and stress-relieved samples of silicon nitride should be the same.

VIII. SUMMARY

We have proposed three possible explanations for the reduction in dissipation due to external and internal stress. These explanations are dissipation dilution, stress increases the tunneling barrier V_0, and stress decreases the TLS-phonon coupling γ. We have used quantitative fits to show that these models are plausible. The only way to determine the respective roles of these effects is to determine the parameters experimentally by measuring the dissipation, thermal conductivity, and specific heat on samples with the same stoichiometry.

It is perhaps useful to view our work in the context of the history to two-level systems and glasses at low temperatures. The original model of two-level systems was proposed by Anderson, Halperin, and Varma, and independently, by W. A. Phillips. It assumed a flat distribution of the asymmetry energy and the tunneling barrier height of two-level systems. This has been an enormously useful model for fitting the low-temperature thermal conductivity, specific heat, dissipation, etc. Tielburger, Merz, Ehrenfels, and Hunklinger used a

Gaussian distribution of the barrier height to extend the model to fit the dissipation over a broader temperature range. Yu and Freeman represented higher energy excitations with Einstein modes to fit the thermal conductivity and specific heat at higher temperatures. Our paper moves the model forward one more step in two ways. First, we show that one set of parameters can be used to fit dissipation, specific heat, and thermal conductivity at both low and high temperatures. Second, we extend the model to include the effect of stress on two-level systems. We propose that stress reduces the effective number of two-level systems, either by increasing the tunneling barrier height or by decreasing the TLS-phonon coupling. As a result, stress would decrease the dissipation and dielectric loss as well as increase the thermal conductivity, which could have important practical applications. Examples include substrates for integrated circuits where cooling is crucial, and superconducting qubits where low dielectric noise is important.

APPENDIX

In this Appendix we show the calculations involved in our estimate of dissipation dilution. We also show the sensitivity of our fits to the values of the parameters.

1. Estimation of the contribution of dissipation dilution

In dissipation dilution[7] materials made stiffer by externally applied stress without increasing their loss have a higher Q. If we write a complex Young's modulus $E = E_0(1 + i\phi)$, where ϕ is the internal friction and E_0 is a constant, then $Q^{-1} = A\phi(\omega_0)$, where A is due to dissipation dilution and ω_0 is the resonant frequency.[5,7,32]

We can estimate the contribution of dissipation dilution to the reduction in dissipation of high-stress silicon nitride by noting that the experimental geometry is that of a thin-film square resonator.[4] The energy of the resonator consists of three parts: the kinetic energy K, the energy V_s from stressing the material, and the elastic energy V_{el}. In this case[5]

$$A = \frac{V_{el}}{V_s + V_{el}} \approx \frac{V_{el}}{V_s} \tag{A1}$$

since, as we shall show, $V_{el} \ll V_s$. We can make the approximation

$$\frac{V_{el}}{V_s} = \left(\frac{f_{0,\text{stress relieved}}}{f_{0,\text{high stress}}}\right)^2, \tag{A2}$$

where f_0 is the fundamental frequency of the resonator. The energy of a square thin-film resonator has three contributions:[33]

$$H = K + V_s + V_{el}, \tag{A3}$$

$$K = \frac{1}{2}\int_0^{L_x}\int_0^{L_y}\rho\,[\dot{u}(x,y)]^2\,dx\,dy, \tag{A4}$$

$$V_s = \frac{1}{2}\int_0^{L_x}\int_0^{L_y}T\left[\left(\frac{\partial u}{\partial x}\right)^2 + \left(\frac{\partial u}{\partial y}\right)^2\right]dx\,dy, \tag{A5}$$

$$V_{el} = \frac{1}{2}\int_0^{L_x}\int_0^{L_y}EI\left[\left(\frac{\partial^2 u}{\partial x^2}\right)^2 + \left(\frac{\partial^2 u}{\partial y^2}\right)^2\right.$$
$$\left. + 2\nu\left(\frac{\partial^2 u}{\partial x^2}\right)\left(\frac{\partial^2 u}{\partial y^2}\right) + 2(1-\nu)\left(\frac{\partial^2 u}{\partial x\partial y}\right)^2\right]dx\,dy, \tag{A6}$$

where $u(x,y)$ is the displacement perpendicular to the x-y plane, $L_x = L_y = L$ are the length of the sides, ρ is the mass per unit area, and E is the Young's modulus. T is the tensile force per unit length given by $T = Sd$, where S is the stress. $I = d^3/12(1-\nu)$, where d is the thickness of the plate and ν is Possion's ratio, which is 0.24 for silicon nitride.[34] The equation of motion for $u(x,y)$ is

$$\rho\frac{d^2u(x,y)}{d^2t} = -EI\left[\frac{\partial^4}{\partial x^4} + \frac{\partial^4}{\partial y^4} + 2\frac{\partial^2}{\partial x^2}\frac{\partial^2}{\partial y^2}\right]u(x,y)$$
$$+ T\left[\frac{\partial^2}{\partial x^2} + \frac{\partial^2}{\partial y^2}\right]u(x,y). \tag{A7}$$
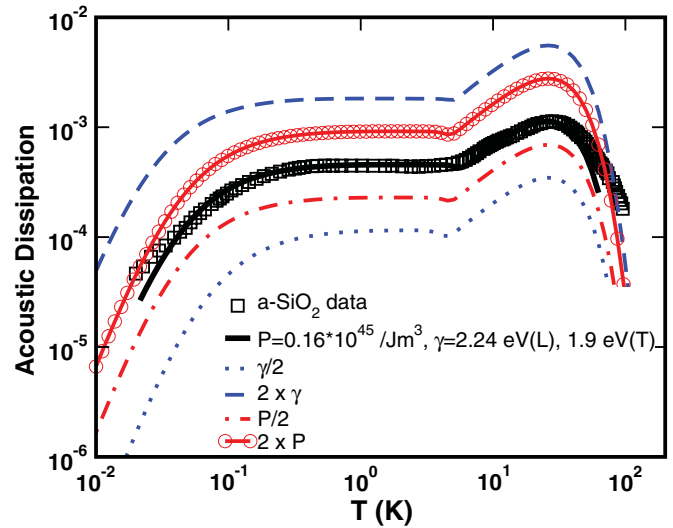

FIG. 5. (Color online) Acoustic dissipation Q^{-1} vs temperature for various values of the deformation potential γ and the TLS density of states $\bar{P}$. The black squares are the SiO$_2$ data measured at 11.4 kHz from Tielburger *et al.*[17] The black solid line is the fit using the values in Table I with $\bar{P} = 0.16 \times 10^{45}/$J m^3, longitudinal $\gamma = 2.24$ eV, and transverse $\gamma = 1.9$ eV. The dotted blue line comes from using values of γ that are half as large, while the dashed blue line comes from multiplying the values of γ by 2. The red dot-dashed line is the result of using a value of $\bar{P}$ that is half as large, while the solid red line with open circles uses a value of $\bar{P}$ that is twice as large.
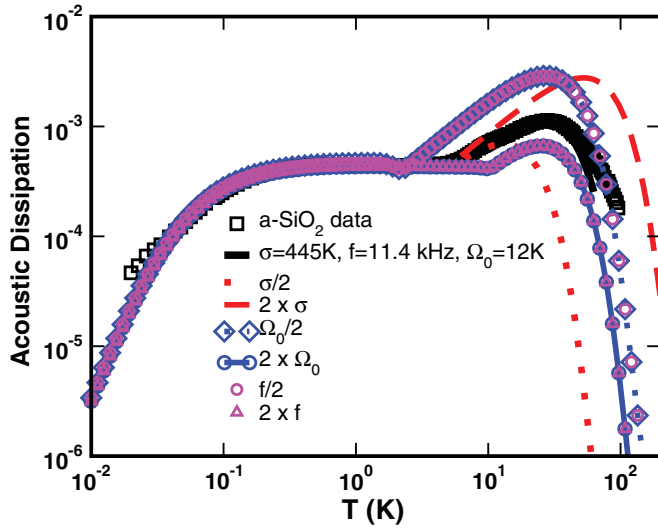
FIG. 6. (Color online) Acoustic dissipation Q^{-1} vs temperature for various values of the width σ of the distribution of the barrier height V, the energy level spacing $\hbar\Omega_0$, and the measuring frequency f. The black squares are the SiO$_2$ data measured at 11.4 kHz from Tielburger *et al.*[17] The black solid line is the fit using the values in Table I with $\sigma = 445$ K, $\Omega_0 = 12$ K, and $f = 11.4$ kHz. The red dotted line uses half that value of σ, while the red dashed line uses twice the value of σ. The blue dotted line with diamonds uses half the value of Ω_0, and the blue solid line with circles uses twice the value of Ω_0. The magenta circles are for half the frequency and the magneta up triangles are for twice the frequency f.

By assuming a solution of the form $u(x,y) = u_0 \exp[ik_x x + ik_y y - i\omega t]$, we find the dispersion relation:

$$\omega = \sqrt{\frac{T}{\rho}k^2 + \frac{EI}{\rho}k^4}, \qquad (A8)$$

where $k^2 = k_x^2 + k_y^2$. With the boundary condition $u(0,y) = u(L,y) = u(x,0) = u(x,L) = 0$, the fundamental mode corresponds to $k_x = k_y = 2\pi/L$ giving the fundamental resonant frequency:

$$
\begin{aligned}
f_0 &= \frac{\omega_0}{2\pi} \\
&= \sqrt{\frac{2S}{\rho_0}\left(\frac{1}{L}\right)^2 + \frac{4E}{12(1-v^2)\rho_0}\left(\frac{2\pi d}{L}\right)^2\left(\frac{1}{L}\right)^2}, \quad (A9)
\end{aligned}
$$

where $\rho_0 = \rho/d$.

We can estimate the fundamental resonant frequencies of a square thin-film resonator made of high-stress and
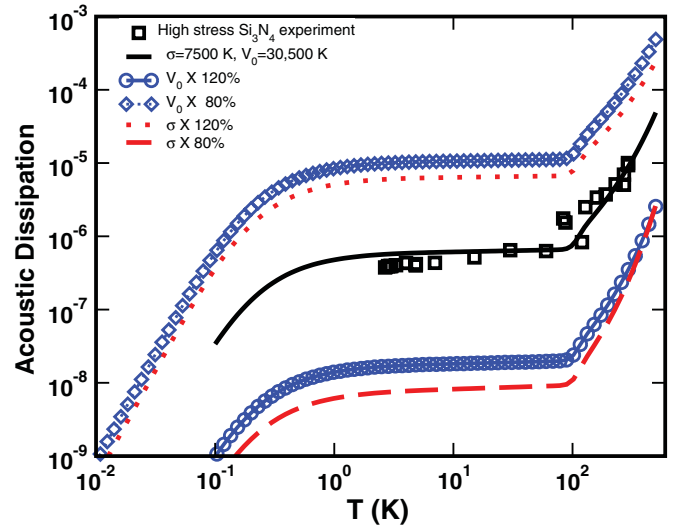

FIG. 7. (Color online) Acoustic dissipation Q^{-1} vs temperature for various values of σ and and V_0. The black squares are the experimental data points for high-stress Si$_3$N$_4$ from Ref. 4. The black solid line shows the fit to the data. We have varied σ and V_0 by 20% above and below the fit values to show the sensitivity of the fit to the values of the parameters. The values of the other parameters are given in Table I.

stress-relieved Si$_3$N$_4$ using values from Ref. 4: $S = 1.2$ GPa for high-stress silicon nitride, $d = 30$ nm, and $L = 255$ μm. The Young's modulus is $E = 300$ GPa,[34] and the mass density is $\rho_0 = 3180$ kg/m^3. We estimate $f_0 \sim 3.4$ MHz for the high-stress resonator compared with the experimental value of 1.526 445 MHz.[4] For the hypothetical stress-relieved resonator with $S = 0$, we estimate $f_0 \sim 17$ kHz. This gives a ratio of $(f_{0,\text{high stress}}/f_{0,\text{stress relieved}}) \sim 200$. Thus from Eqs. (A1) and (A2) $A \sim 2.5 \times 10^{-5}$, i.e., Q is enhanced up to a factor of 40 000 by dissipation dilution. However, experimentally,[4] the Q of high-stress silicon nitride is increased by a factor of order 150 by external stress. The full enhancement of 40 000 is not realized, probably due to external sources of dissipation, e.g., clamping losses.

2. Sensitivity of fits to parameters

To show the sensitivity of our fits to the parameters $\bar{P}$, γ, σ, Ω, and the frequency f, we show in Figs. 5, 6, and 7 how the dissipation would change if we varied these parameters by a factor of 2 from the values that we quoted in Table I in the paper.

[1] R. C. Zeller and R. O. Pohl, Phys. Rev. B **4**, 2029 (1971).

[2] R. O. Pohl, X. Liu, and E. Thompson, Rev. Mod. Phys. **74**, 991 (2002).

[3] X. Liu, B. E. White, R. O. Pohl, E. Iwanizcko, K. M. Jones, A. H. Mahan, B. N. Nelson, R. S. Crandall, and S. Veprek, Phys. Rev. Lett. **78**, 4418 (1997).

[4] D. R. Southworth, R. A. Barton, S. S. Verbridge, B. Ilic, A. D. Fefferman, H. G. Craighead, and J. M. Parpia, Phys. Rev. Lett. **102**, 225503 (2009).

[5] P. R. Saulson, Phys. Rev. D **42**, 2437 (1990).

[6] P. R. Saulson (private communication).

[7] Y. L. Huang and P. R. Saulson, Rev. Sci. Instrum. **69**, 544 (1998).

[8] W. A. Phillips, J. Low Temp. Phys. **7**, 351 (1972).

[9] P. W. Anderson, B. I. Halperin, and C. M. Varma, Philos. Mag. **25**, 1 (1972).

[10] J. Jackle, Z. Phys. **257**, 212 (1972).

[11] J. Jackle, L. Piche, W. Arnold, and S. Hunklinger, J. Non-Cryst. Solids **20**, 365 (1976).

[12]S. Hunklinger and A. K. Raychaudhuri, Prog. Low Temp. Phys. **9**, 265 (1986).

[13]S. Hunklinger and W. Arnold, in *Physical Acoustics: Principles and Methods*, edited by W. P. Mason and R. N. Thurston, Vol. 12 (Academic, New York, 1976), pp. 155–215.

[14]S. Hunklinger and M. v. Schickfus, in *Amorphous Solids* (Springer-Verlag, New York, 1981), p. 81.

[15]J. M. Martinis, K. B. Cooper, R. McDermott, M. Steffen, M. Ansmann, K. D. Osborn, K. Cicak, S. Oh, D. P. Pappas, R. W. Simmonds, and C. C. Yu, Phys. Rev. Lett. **95**, 210503 (2005).

[16]H. Paik and K. D. Osborn, Appl. Phys. Lett. **96**, 072505 (2010).

[17]D. Tielburger, R. Merz, R. Ehrenfels, and S. Hunklinger, Phys. Rev. B **45**, 2750 (1992).

[18]R. J. Nemanich, Phys. Rev. B **16**, 1655 (1977); E. Duval, A. Boukenter, and B. Champagnon, Phys. Rev. Lett. **56**, 2052 (1986); A. P. Sokolov, A. Kisliuk, M. Soltwisch, and D. Quitmann, *ibid.* **69**, 1540 (1992).

[19]C. C. Yu and J. J. Freeman, Phys. Rev. B **36**, 7620 (1987).

[20]J. J. Freeman and A. C. Anderson, Phys. Rev. B **34**, 5684 (1986).

[21]M. P. Zaitlin and A. C. Anderson, Phys. Rev. B **12**, 4475 (1975).

[22]M. v. Schickfus and S. Hunklinger, Phys. Lett. A **64**, 144 (1977).

[23]A. D. Fefferman, R. O. Pohl, A. T. Zehnder, and J. M. Parpia, Phys. Rev. Lett. **100**, 195501 (2008).

[24]C. C. Yu, J. Low Temp. Phys. **137**, 251 (2004).

[25]D. R. Queen and F. Hellman, Rev. Sci. Instrum. **80**, 063901 (2009).

[26]J. C. Lasjaunias, A. Ravex, and M. Vandorpe, Solid State Commun. **17**, 1045 (1975).

[27]T. L. Smith, Ph.D. thesis, University of Illinois, 1975.

[28]Y. S. Touloukian, R. W. Powell, C. Y. Ho, and P. G. Klemens, in *Thermophysical Properties of Matter*, Vol. 2 (Plenum, New York, 1970), p. 193.

[29]L. Martin-Moreno, E. Martinez, J. A. Verges, and F. Yndurain, Phys. Rev. B **35**, 9683 (1987).

[30]M. F. Thorpe, J. Non-Cryst. Solids **53**, 355 (1983).

[31]J. Robertson, Eur. Phys. J. Appl. Phys. **28**, 265 (2004).

[32]G. I. González and P. R. Saulson, J. Acoust. Soc. **96**, 207 (1994).

[33]S. Timoshenko, *Vibration Problems in Engineering*, 2nd ed. (D. Van Nostrand, New York, 1937).

[34]K. B. Gavan, H. J. R. Westra, E. W. J. M. van der Drift, W. J. Venstra, and H. S. J. van der Zant, Appl. Phys. Lett. **94**, 233108 (2009).